HAL
archives-ouvertes.fr

Shape optimization for inverse electromagnetic casting problems (version longue)

Alfredo Canelas, Jean Rodolphe Roche, Jose Herskovits

▶ **To cite this version:**

Alfredo Canelas, Jean Rodolphe Roche, Jose Herskovits. Shape optimization for inverse electromagnetic casting problems (version longue). 2010. <inria-00533699>

HAL Id: inria-00533699
https://hal.inria.fr/inria-00533699

Submitted on 8 Nov 2010

HAL is a multi-disciplinary open access archive for the deposit and dissemination of scientific research documents, whether they are published or not. The documents may come from teaching and research institutions in France or abroad, or from public or private research centers.

L'archive ouverte pluridisciplinaire **HAL**, est destinée au dépôt et à la diffusion de documents scientifiques de niveau recherche, publiés ou non, émanant des établissements d'enseignement et de recherche français ou étrangers, des laboratoires publics ou privés.

SHAPE OPTIMIZATION FOR INVERSE ELECTROMAGNETIC CASTING PROBLEMS

Alfredo Canelas
Instituto de Estructuras y Transporte
Facultad de Ingeniera, UDELAR
Montevideo, Uruguay
acanelas@fing.edu.uy

Jean R. Roche
Institut Elie Cartan de Nancy
Nancy-Université, CNRS, INRIA
Vandoeuvre lès Nancy, France
roche@iecn.u-nancy.fr

José Herskovits
Mechanical Eng. Program
COPPE - UFRJ,CT
Rio de Janeiro, Brazil
jose@optimize.ufrj.br

ABSTRACT

In this paper we present an algorithm for inverse optimization problems concerning electromagnetic casting of molten metals. We are interested in locating suitable inductors around the molten metal so that the equilibrium shape be as near as possible to a desired target shape. A Simultaneous Analysis and Design (SAND) mathematical programming formulation is stated for the inverse problem. The resulting optimization problem is solved with FAIPA, a feasible directions interior-point algorithm.

INTRODUCTION

The industrial technique of electromagnetic casting allows for contactless heating, shaping and controlling of chemical aggressive, hot melts. The main advantage over the conventional crucible shape forming is that the liquid metal does not come into contact with the crucible wall, so there is no danger of contamination. This is very important in the preparation of very pure specimens in metallurgical experiments, as even small traces of impurities, such as carbon and sulphur, can affect the physical properties of the sample. Industrial applications are, for example, electromagnetic shaping of aluminum ingots using soft-contact confinement of the liquid metal, electromagnetic shaping of components of aeronautical engines made of superalloy materials (Ni,Ti, ...), control of the structure solidification, etc.

The direct problem is to determine the resulting liquid metal shape for a given external current distribution. The model considered here concerns a vertically falling molten metal column shaped by an externally applied magnetic field created by a set of inductors. In general, the direct problem can be solved either directly studying the equilibrium equation at the interface, or minimizing an appropriate energy functional, the main advantage of this last method being that the resulting shapes are then mechanically stable [1, 2, 3].

The inverse problem consists in determining the exterior field, and therefore the external currents, for which the liquid metal takes on a given desired shape. In the two-dimensional case, the inverse shaping problem consists in finding a distribution of inductors in order that the generated exterior field makes the horizontal cross-section of the molten metal attain a prescribed shape. This is a very important problem that one needs to solve in order to define a process of electromagnetic liquid metal forming. In addition, from a practical point of view, the magnetic field has to be created by a simple configuration of inductors.

The direct problem is inherently well posed, i.e. small variations in the applied currents cause small variations in the shape. The inverse problem is inherently ill posed: small variation of the liquid boundary may cause dramatic variations in the applied exterior field [4, 5].

In a previous work we studied the inverse electromagnetic shaping problem considering the case where the inductors are made of single solid-core wires with a negligible area of the cross-section [6]. Thus, the inductors were represented by points in the horizontal plane. In a second paper we considered the more realistic case where each inductor is a set of bundled insulated strands [7].

In the present paper we introduce a regularized cost function in order to treat the numerical instability. The most important effect of the regularization term is to control the magnetic pressure in the boundary of the computed shape. Thus, this term ensures that the boundary of the liquid metal is smooth.

Two different approaches are considered, the first one seeks for a set of inductors such that the distance between the equilibrium shape and the given target one is minimized. The second approach looks for a set of inductors such that a slack function related to the equilibrium relation on the boundary of the target shape is minimized.

A SAND mathematical programming method is stated for both inverse problem formulations. This method considers the position of the inductors, shape parameters and state variables as unknowns, see [8, 9]. The obtained optimization problems are solved employing FAIPA [10, 11], a feasible directions interior point algorithm.

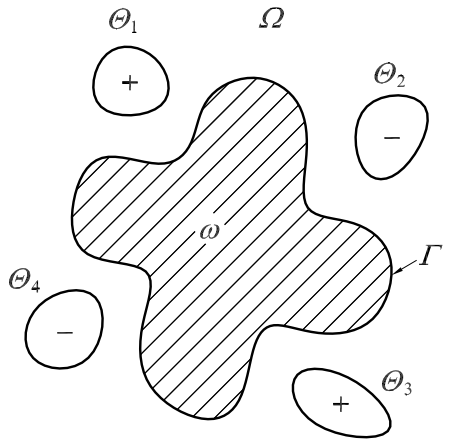

Figure 1. Direct electromagnetic casting problem.

THE MATHEMATICAL MODEL

The model

The simplified model of the electromagnetic shaping problem studied here concerns the case of a vertical column of liquid metal falling down into an electromagnetic field created by vertical inductors. We assume that the frequency of the imposed current is very high so that the magnetic field does not penetrate into the metal. In other words, we neglect the skin effect. Moreover, we assume that a stationary horizontal section is reached so that the 2-dimensional model is valid. The equilibrium of the system is ensured by the static balance on the surface of the metal between the surface tension and the electromagnetic forces. This problem and other similar ones have been considered by several authors, we refer the reader to the following papers for the physical analysis of the simplifying assumptions of the model: see [12, 13, 4, 1, 14, 15, 2].

We denote by Ω the exterior in the plane of the closed and simply connected domain ω occupied by the cross-section of the metal column. The exterior magnetic field can be found as the solution of the following boundary value problem:

$$\begin{aligned}
\nabla\times\boldsymbol{B} &= \mu_0\boldsymbol{J} && \text{in } \Omega, && (1)\\
\nabla\cdot\boldsymbol{B} &= 0 && \text{in } \Omega, && (2)\\
\boldsymbol{B}\cdot\nu &= 0 && \text{on } \Gamma, && (3)\\
\|\boldsymbol{B}(x)\| &= O(\|x\|^{-1}) && \text{as } \|x\|\to\infty \text{ in } \Omega && (4)
\end{aligned}$$

Here the fields $\boldsymbol{J} = (0, 0, j_0)$ and $\boldsymbol{B} = (B_1, B_2, 0)$ represent the mean square values of the current density vector and the total magnetic field, respectively. The constant μ_0 is the vacuum permeability, ν the unit normal vector to the boundary Γ and $\|\cdot\|$ denotes the Euclidean norm. We assume that j_0 has compact support in Ω and satisfies:

$$\int_\Omega j_0\,dx = 0. \tag{5}$$

Since it is assumed that the molten metal is incompressible, we have the following condition:

$$\int_\omega dx = S_0, \tag{6}$$

where S_0 is given.

On the other hand, the magnetic field produces a surface pressure that acts on the liquid metal changing its shape until the equilibrium is attained. The equilibrium is characterized by the following equation [15, 16]:

$$\frac{1}{2\mu_0}\|\boldsymbol{B}\|^2 + \sigma\mathcal{C} = p_0 \quad \text{on } \Gamma, \tag{7}$$

where $\mathcal{C}$ is the curvature of Γ seen from the metal, σ is the surface tension of the liquid and the constant p_0 is an unknown of the problem. Physically, p_0 represents the difference between the internal and external pressures.

In the direct problem the electric current density J is given and one needs to find the shape of ω that satisfies (6) and such that the magnetic field $\boldsymbol{B}_\omega$ solution of (1)-(4) satisfies also the equilibrium equation (7) for a real constant p_0.

Conditions (1)-(5), with the function j_0 compactly supported in Ω, imply that there exists the flux function $\varphi : \Omega \to \mathbb{R}$ such that
$\boldsymbol{B} = (\frac{\partial \varphi}{\partial x_2}, -\frac{\partial \varphi}{\partial x_1}, 0)$ with φ solution of:

$$\begin{array}{rll} -\Delta\varphi & = \mu_0 j_0 & \text{in } \Omega, \\ \varphi & = 0 & \text{on } \Gamma, \\ \varphi(x) & = O(1) & \text{as } \|x\| \to \infty. \end{array} \tag{8}$$

The equilibrium equation (7) in terms of the flux becomes:

$$\frac{1}{2\mu_0} \left| \frac{\partial \varphi}{\partial \nu} \right|^2 + \sigma \mathcal{C} = p_0 \quad \text{on } \Gamma. \tag{9}$$

The direct problem, in terms of the flux, consists in looking for a domain ω such that the solution φ of (8) satisfies (9) for a real constant p_0.

Variational formulation

Under suitable assumptions, the equilibrium configurations are given by the local stationary points with respect to the domain of the following total energy:

$$E(\omega) = -\frac{1}{2\mu_0} \int_\Omega \left| \frac{\partial \varphi_\omega}{\partial \nu} \right|^2 dx + \sigma P(\omega), \tag{10}$$

subject to the equality constraint in the measure of ω:

$$\int_\omega dx \quad = \quad S_0. \tag{11}$$

where in (10), we have been used the notation φ_ω for the solution of (8), with the purpose of highlighting the dependence of the flux with respect to the domain ω. $P(\omega)$ is the perimeter of ω, i.e., the length of $\Gamma = \partial\omega$ when $\partial\omega$ is regular enough (for instance of class C^1):

$$P(\omega) = \int_\Gamma d\gamma, \tag{12}$$

where $d\gamma =$ length measure on Γ.

The variational formulation of the direct problem consists in finding the domain ω as a stationary point of the total energy (10), subject to the constraint (11). As φ_ω is solution of (8), to prove that this variational formulation is equivalent to the previous one it remains to show that the equilibrium relation is automatically ensured for all the stationary points.

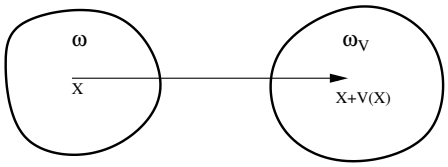

Figure 2. Domain perturbation.

First order optimality conditions

In this section we derive the necessary condition for a domain ω to be a stationary point of the total energy (10), subject to the constraint (11). For that purpose we consider shape derivatives. Differentiation with respect to the domain is a classical issue, in this work we consider the point of view of F. Murat and J. Simon; see [17, 18, 19].

Let $V \in W^{1,\infty}(\mathbb{R}^2, \mathbb{R}^2)$ the set of the Lipschitz functions ϕ from $\mathbb{R}^2$ to $\mathbb{R}^2$ such that ϕ and $\nabla\phi$ are uniformly bounded [17]. Let ω be a bounded domain in $\mathbb{R}^2$ of class C^2. We consider a shape deformation given by the mapping $Id + V$, where Id is the identity mapping. Then, the deformed domain ω_V is defined by $\omega_V = \{x + V(x) \mid x \in \omega\}$; see Fig. 2.

For every $V \in W^{1,\infty}(\mathbb{R}^2, \mathbb{R}^2)$ the mapping $Id + V$ is a diffeomorphism provided $\|V\|_{W^{1,\infty}(\mathbb{R}^2,\mathbb{R}^2)} < 1$ [17].

Let $\mathcal{O}(\omega)$ be the collection of images of ω considering all possible diffeomorphisms. If F is a scalar function defined in $\mathcal{O}(\omega)$ we say that it is shape differentiable if the function $V \to F(\omega_V)$ is differentiable at $V = 0$ in the Banach space $W^{1,\infty}(\mathbb{R}^2, \mathbb{R}^2)$.

The derivative of F, defined in $W^{1,\infty}(\mathbb{R}^2, \mathbb{R}^2)$, is called *shape gradient* and is denoted by $F'(\omega)$. It can be shown that the linear application $V \to F'(\omega)(V)$ is determined by the normal component of V in the boundary of ω, see [17], [20] and [14] for a detailed description of the shape derivative structure.

Let L be the Lagrangian function defined in $\mathcal{O}(\omega) \times \mathbb{R}$ by:

$$L(\omega, p_0) = E(\omega) - p_0(m(\omega) - S_0), \tag{13}$$

Then, the first order optimality condition is the following:

$$L'(\omega, p_0)(V) = 0 \quad \forall V \in W^{1,\infty}(\mathbb{R}^2, \mathbb{R}^2). \tag{14}$$

This kind of optimality conditions often appear in hydrodynamic problems and other fluid problems; let us refer for instance to reference [2] where a large class of liquid metal equilibria is considered.

The next theorem shows how the term $L'(\omega, p_0)(V)$ of (14) can be calculated.

Theorem

Let Ω be the complement of a compact set ω in $\mathbb{R}^2$ with nonempty interior. Assume that $\Gamma = \partial\omega = \partial\Omega$ is of class C^2. Let V be in $W^{1,\infty}(\mathbb{R}^2, \mathbb{R}^2)$ with compact support and $\|V\|_{W^{1,\infty}(\mathbb{R}^2,\mathbb{R}^2)} < 1$. Let j_0 be a square integrable function from Ω into $\mathbb{R}$ with compact support in Ω.

Then, there exists a unique solution φ_{ω_V} in $C^1(\overline{\Omega}_V)$ (see [21] and [4]) of:

$$\begin{array}{rll} -\Delta\varphi_{\omega_V} & = \mu_0 j_0 & \text{in } \Omega_V, \\ \varphi_{\omega_V} & = 0 & \text{on } \partial\Omega_V, \\ \varphi_{\omega_V}(x) & = O(1) & \text{as } \|x\| \to \infty. \end{array} \tag{15}$$

and the shape derivative of the lagrangian L is given by:

$$\begin{aligned} L'(\omega, p_0)(V) &= \int_\Gamma \left(\frac{1}{2\mu_0} \left| \frac{\partial\varphi_\omega}{\partial\nu} \right|^2 \right) (V \cdot \nu)\, d\gamma \\ &+ \int_\Gamma (\sigma\mathcal{C} - p_0)\, (V \cdot \nu)\, d\gamma, \end{aligned}$$

where ν is the unit normal to Γ oriented toward Ω, $\mathcal{C}$ is the curvature of Γ (seen from the metal) and φ_ω the solution of (8).$\diamond$

See [4, 15, 14, 17].

THE INVERSE PROBLEM

The goal of the inverse problem is to find a distribution of current around the liquid metal column so that it attains a given shape. This topic was already studied and there are a few number of papers about the existence of such solutions. See [4, 5].

It has been shown that the magnetic field $\boldsymbol{B}$ is the unique analytic extension of the field $\boldsymbol{B}\cdot\tau$ defined on the boundary Γ of the liquid metal (τ being the unit tangent vector to Γ) [4]. Furthermore, from (7) and (9), it is possible to show the following:

$$\boldsymbol{B}\cdot\tau = \epsilon\sqrt{p_0 - \sigma\mathcal{C}} \quad \text{with} \quad \epsilon = \pm 1\,. \tag{16}$$

The constant p_0 must be such that:

$$p_0 \geq \max_\Gamma \sigma\mathcal{C}\,. \tag{17}$$

In [4], the authors proved that a solution for $\boldsymbol{B}$ exists only if Γ is an analytic curve, and the function $\boldsymbol{B}\cdot\tau$ is analytic. If $p_0 > \max_\Gamma \sigma\mathcal{C}$ then ϵ is constant on Γ. So if we have $p_0 = \max_\Gamma \sigma\mathcal{C}$ another restriction is imposed on Γ since ϵ change sign around points where $\boldsymbol{B}.\tau = 0$ (i.e. where $\mathcal{C}$ attaints it maximum), depending on the multiplicity order of these zero points: if the multiplicity order of a zero point is even, ϵ remains constant in its neighborhood. On the other hand if the multiplicity order of a zero point is odd, ϵ will change sign. Hence by periodicity the number of singular points of odd order must be even. For example any curve which has its curvature attaining its maximum value at an odd number of points (at which $\boldsymbol{B}.\tau$ has non-degenerate zeros), is in fact impossible to form.

In the present approach, given the target shape ω^*, we look for a electric current density j_0 as the solution of the following optimization problem:

$$\min_{j_0} \; d(\omega, \omega^*), \tag{18}$$

where $d(\omega, \omega^*)$ is a "distance" between ω and ω^*, see [17]. The domain ω belongs to the set of admissible domains, i.e., $\omega \in \mathcal{O}(\omega^*)$, and satisfies the first order optimality condition (14) under the action of the electric current density j_0.

In addition, the magnetic field has to be created by a simple configuration of inductors. Hence we consider a distribution of the electric current density j_0 of the form:

$$j_0 = I \sum_{p=1}^{m} \alpha_p \chi_{\Theta_p}, \tag{19}$$

where I is a given intensity of current, Θ_p, with $1 \leq p \leq m$, are inductors of circular cross-section, χ_{Θ_p} are their characteristic functions, and α_p are dimensionless coefficients. Then, the inverse problem consists in determining the position and radius of the circles Θ_p. Thus, we have to solve a finite dimensional optimization problem with $3m$ project variables.

Note that the expression (19) assumes that the electric current density is uniform on each region Θ_p. Inductors made of bundled insulated strands allow the use of (19) as a good approximation, see [22] and references therein.

To find an approximate solution of problem (18) we considers a domain deformation of ω^*

defined by the diffeomorphism $Id + Z$, with $Z \in W^{1,\infty}(\mathbb{R}^2, \mathbb{R}^2)$. Then denoting T_Z the mapping:

$$T_Z(x) = x + Z(x)\,, \tag{20}$$

we define:

$$\begin{aligned} \omega_Z &= T_Z(\omega^*)\,, \\ \Gamma_Z &= T_Z(\Gamma^*)\,. \end{aligned}$$

The first formulation of the inverse problem that is considered here is:

$$\begin{aligned} &\min_{j_0, Z} \|Z\|^2_{L^2(\Gamma^*)} + r \left\| \frac{\partial \varphi_\omega}{\partial \nu} \right\|^2_{L^2(\Gamma^*)}\,, \\ &\text{subject to:} \\ &\omega_Z \text{ is in equilibrium under } j_0. \end{aligned} \tag{21}$$

where $\left\| \frac{\partial \varphi_\omega}{\partial \nu} \right\|^2_{L^2(\Gamma^*)}$ is a penalty term, and r is a positive parameter. The regularization term penalize solutions presenting a high magnetic pressure in the shape boundary. Hence the computed solutions to the inverse problem will give a magnetic field corresponding to a smooth boundary Γ^*.

The equilibrium of ω_Z is understood in the variational sense, i.e.,

$$\begin{aligned} &\int_{\Gamma_Z} \left(\frac{1}{2\mu_0} \left| \frac{\partial \varphi_{\omega_Z}}{\partial \nu} \right|^2 \right) (V \cdot \nu)\; d\gamma \\ + \quad &\int_{\Gamma_Z} (\sigma \mathcal{C} - p_0)\,(V \cdot \nu)\; d\gamma = 0 \\ \forall \quad &V \text{ in } W^{1,\infty}(\mathbb{R}^2, \mathbb{R}^2)\,. \end{aligned} \tag{22}$$

A second formulation of the inverse problem can be considered if we introduce a slack variable function $p(x) : \Gamma^* \to \mathbb{R}$ in the equilibrium equation. That is, we say that ω^* is in equilibrium under j_0 and p if

$$\begin{aligned} &\int_{\Gamma^\star} \left(\frac{1}{2\mu_0} \left| \frac{\partial \varphi_{\omega^\star}}{\partial \nu} \right|^2 \right) (V \cdot \nu)\; d\gamma \\ + \quad &\int_{\Gamma^\star} (\sigma \mathcal{C} - p_0 + p)\,(V \cdot \nu)\; d\gamma = 0 \\ \forall \quad &V \text{ in } W^{1,\infty}(\mathbb{R}^2, \mathbb{R}^2)\,, \end{aligned} \tag{23}$$

where φ_{ω^*} is the solution of the state equation (8) in Ω^*. Then, we obtain the following formulation of the problem:

$$\begin{aligned} &\min_{j_0, p} \|p\|^2_{L^2(\Gamma^*)} + r \left\| \frac{\partial \varphi_\omega}{\partial \nu} \right\|^2_{L^2(\Gamma^*)}\,, \\ &\text{subject to:} \\ &\omega^* \text{ is in equilibrium under } j_0 \text{ and } p. \end{aligned} \tag{24}$$

Note that in this formulation the shape of the liquid metal is no more an unknown of the optimization problem.

NUMERICAL METHOD

The exterior Dirichlet problem

To solve (8) in the exterior domain Ω we consider a particular solution φ_1 of the differential equation given by:

$$\varphi_1(x) = -\frac{\mu_0}{2\pi} \int_{\mathbb{R}^2} \ln \|x - y\| j_0(y)\, dy. \tag{25}$$

This function is a solution of the problem:

$$-\Delta \varphi_1(x) = \mu_0 j_0 \quad \text{in } \mathbb{R}^2, \tag{26}$$

$$\varphi_1(x) = O(1) \quad \text{as } \|x\| \to \infty. \tag{27}$$

Note that for the current density distribution defined by (19), the expression of φ_1 is

$$\varphi_1(x) = -\frac{\mu_0 I}{2\pi} \sum_{p=1}^{m} \alpha_p \int_{\Theta_p} \ln \|x - y\|\, dy. \tag{28}$$

The function φ_1 can be calculated as a sum of line integrals on the boundaries Γ_p of domains Θ_p. Consider the function $w : \mathbb{R}^2 \times \mathbb{R}^2 \to \mathbb{R}^2$ defined as:

$$w(x, y) = (1/4)(1 - 2 \ln \|x - y\|)(x - y). \tag{29}$$

The divergence of w is $\nabla_y \cdot w = \ln \|x - y\|$. Then, (28) becomes:

$$\varphi_1(x) = -\frac{\mu_0 I}{2\pi} \sum_{p=1}^{m} \alpha_p \int_{\Gamma_p} w(x, y) \cdot \nu\, d\gamma. \tag{30}$$

The function φ can be computed as:

$$\varphi(x) = \xi(x) + \varphi_1(x), \tag{31}$$

where the function ξ is the solution of the following exterior problem:

$$\begin{aligned} -\Delta \xi(x) &= 0 && \text{in } \Omega, \\ \xi(x) &= -\varphi_1(x) && \text{on } \Gamma, \\ \|\xi(x)\| &= O(1) && \text{as } \|x\| \to \infty. \end{aligned} \tag{32}$$

Following Kress [21], an integral single layer representation of the solution of (32) is given by:

$$\xi(x) = -\frac{1}{2\pi}\int_\Gamma q(y)\ln\|x-y\|\,d\gamma + c, \quad (33)$$

where the constant c is the value at the infinity of ξ and the function $q(y) \in H^{-1/2}(\Gamma)$ satisfies:

$$\int_\Gamma q(y)\,d\gamma = 0. \quad (34)$$

It remains to impose the boundary conditions on Γ. Here, this is done with a weak formulation. Let $a_\Gamma(q,g)$ be the following elliptic bilinear form:

$$\begin{aligned} &a_\Gamma(q,g) = \\ &= -\frac{1}{2\pi}\int_\Gamma g(x)\int_\Gamma q(y)\ln\|x-y\|\,d\gamma\,d\gamma \\ &+c\int_\Gamma g(x)\,d\gamma \end{aligned} \quad (35)$$

defined on $H^{-1/2}(\Gamma)\times H^{-1/2}(\Gamma)$. We look for a function $q(y) \in H^{-1/2}(\Gamma)$ that satisfies (34) and:

$$a_\Gamma(q,g) = -\int_\Gamma \varphi_1(x)g(x)\,d\gamma \quad \forall\, g \in H^{-1/2}(\Gamma). \quad (36)$$

Equation (36) with φ_1 given by (30) will be used instead of (8). Note that the unknown variables are now the function q and the scalar c.

Finally, $\left|\frac{\partial\varphi}{\partial\nu}\right|$ in the equilibrium equation (22) can be computed as:

$$\left|\frac{\partial\varphi}{\partial\nu}\right| = \left|\frac{\partial\varphi_1}{\partial\nu} + \frac{\partial\xi}{\partial\nu}\right|, \quad (37)$$

where the normal derivative of φ_1 is obtained from (30):

$$\frac{\partial\varphi_1}{\partial\nu_x}(x) = -\frac{\mu_0 I}{2\pi}\sum_{p=1}^{m}\alpha_p\int_{\Gamma_p}\frac{\partial}{\partial\nu_x}(w(x,y)\cdot\nu)\,d\gamma. \quad (38)$$

The following expression can be used for ξ:

$$\frac{\partial\xi}{\partial\nu_x}(x) = -\frac{1}{2\pi}\int_\Gamma q(y)\frac{\partial}{\partial\nu_x}\ln\|x-y\|\,d\gamma + \frac{1}{2}q(x), \quad (39)$$

for all $x \in \Gamma$, where the integral of (39) is understood in the Cauchy principal value sense.

The SAND formulation of the inverse problems

A SAND formulation of the inverse problems (21) and (24) is employed here. In other words, the state variables, c and q are incorporated as unknowns of the optimization problem and the state and equilibrium equations are incorporated as equality constraints. The optimization problem of the formulation (21) becomes:

$$\min_{j_0,Z,c,q}\|Z\|^2_{L^2(\Gamma^*)} + r\left\|\frac{\partial\varphi_\omega}{\partial\nu}\right\|^2_{L^2(\Gamma^*)}, \quad (40)$$

subject to the area constraint:

$$\int_{\omega_Z} dx = S_0, \quad (41)$$

the state equations:

$$\begin{aligned} a_{\Gamma_Z}(q,g) &= -\int_{\Gamma_Z}\varphi_1(x)g(x)\,d\gamma \\ &\forall \quad g \in H^{-1/2}(\Gamma_Z), \end{aligned} \quad (42)$$

$$\int_{\Gamma_Z} q(y)\,d\gamma = 0, \quad (43)$$

and the equilibrium equation:

$$\begin{aligned} &\int_{\Gamma_Z}\left(\frac{1}{2\mu_0}\left|\frac{\partial\varphi_\omega}{\partial\nu}\right|^2\right)(V\cdot\nu)\,d\gamma \\ &+ \int_{\Gamma_Z}(\sigma\mathcal{C}-p_0)\,(V\cdot\nu)\,d\gamma = 0 \\ &\forall \quad V \text{ in } C^1(\mathbb{R}^2,\mathbb{R}^2), \end{aligned} \quad (44)$$

where φ_1, φ, and ξ are given by (25), (31) and (33).

The optimization problem of the formulation (24) becomes:

$$\min_{j_0,p,c,q}\|p\|^2_{L^2(\Gamma^*)} + r\left\|\frac{\partial\varphi_\omega}{\partial\nu}\right\|^2_{L^2(\Gamma^*)}, \quad (45)$$

subject to the state equations:

$$\begin{aligned} a_{\Gamma^*}(q,g) &= -\int_{\Gamma^*}\varphi_1(x)g(x)\,d\gamma \\ &\forall \quad g \in H^{-1/2}(\Gamma^*), \end{aligned} \quad (46)$$

$$\int_{\Gamma^*} q(y)\,d\gamma = 0, \quad (47)$$

and the equilibrium equation:

$$\int_{\Gamma^*} \left(\frac{1}{2\mu_0} \left| \frac{\partial \varphi_\omega}{\partial \nu} \right|^2 \right) (V \cdot \nu)\, d\gamma + \int_{\Gamma^*} (\sigma \mathcal{C} - p_0 + p)\, (V \cdot \nu)\, d\gamma = 0 \quad \forall \quad V \text{ in } C^1(\mathbb{R}^2, \mathbb{R}^2), \tag{48}$$

The numerical model

Discretization of the domain

We consider an approximation of the domain ω^* defined by the piecewise linear closed boundary Γ^h, i.e., Γ^h is the union of the n linear finite elements ℓ_j in $\mathbb{R}^2$, $j \in \{1, \ldots, n\}$. The nodes of the boundary Γ^h are denoted by x_i.

A direction $\hat{Z}^i \in \mathbb{R}^2$ is associated to each vertex x_i of Γ^h. We construct a continuous piecewise linear vector field Z^i from Γ^h in $\mathbb{R}^2$ such that $Z^i(x_k) = \delta_{ik} \hat{Z}^i$. The support of Z^i is equal to the union of the finite elements for which x_i is a node. The vector field Z of (20) is computed as:

$$Z(x) = \sum_{i=1}^{n} u_i Z^i(x), \tag{49}$$

and the updated boundary $\Gamma_{\boldsymbol{u}}$ is then given by:

$$\Gamma_{\boldsymbol{u}} = \left\{ X \mid X = x + Z(x);\ u_i \in \mathbb{R},\ x \in \Gamma^h \right\}, \tag{50}$$

where $\boldsymbol{u}^T = (u_1, \ldots, u_n) \in \mathbb{R}^n$ is the vector of unknowns which determine the evolution of the boundary. This representation has the advantage of defining only one degree of freedom for each node. We denote by $\omega_{\boldsymbol{u}}$ the interior domain related to $\Gamma_{\boldsymbol{u}}$ in order to show the dependence with respect to the vector $\boldsymbol{u}$.

Inductors

We consider inductors with a transversal cross-section $\Theta_p = \{x \in \mathbb{R}^2 : \|x - y_p\| \leq \eta\}$, with η a positive real unknown. The contribution of each inductor to the function φ_1 is calculated using (30). The entire set of shape parameters corresponding to the inductors is denoted by $\boldsymbol{u}_p$.

Exterior boundary value problem

For numerical calculations we consider a piecewise constant approximation $q_h(x)$ of $q(x)$:

$$q_h(x) = \sum_{j=1}^{n} q_j e_j(x), \tag{51}$$

where $e_j(x) = 1$ if $x \in \ell_j$ and zero elsewhere.

Replacing the function g in (42) by e_i, with $i \in \{1, \ldots, n\}$, the weak formulation of the boundary value problem, given by equations (42) and (43), becomes:

$$\mathbf{A}(\mathbf{u})\mathbf{q} = \mathbf{b}(\mathbf{u_p}, \mathbf{u}), \tag{52}$$

where the vector $\boldsymbol{q}^T = (q_1, \ldots, q_n, c)$ is in $\mathbb{R}^{n+1}$, $\boldsymbol{u}$ is the vector of shape variables and $\boldsymbol{u}_p$ is the vector that contains the shape parameters of the inductors. The coefficients a_{ij} of the symmetric matrix $\mathbf{A}(\mathbf{u})$ are:

$$a_{ij}(\boldsymbol{u}) = -\frac{1}{2\pi} \int_{\ell_i} \int_{\ell_j} \ln \|x - y\|\, d\gamma\, d\gamma \qquad i, j \in \{1, \ldots, n\}, \tag{53}$$

$$a_{ij}(\boldsymbol{u}) = \int_{\ell_j} d\gamma \qquad i = n+1, \quad \text{and} \quad j \in \{1, \ldots, n\}, \tag{54}$$

and the components b_i of the vector $\boldsymbol{b}$ are:

$$b_i(\boldsymbol{u}_p, \boldsymbol{u}) = -\int_{\ell_i} \varphi_1(x)\, d\gamma \qquad i \in \{1, \ldots, n\}, \tag{55}$$

$$b_i(\boldsymbol{u}_p, \boldsymbol{u}) = 0 \quad i = n+1. \tag{56}$$

For given vectors $\boldsymbol{u}$ and $\boldsymbol{u}_p$, the linear system (52) is symmetric and non-sparse. Numerical approximations of the element integrals of previous and later equations are computed by Gauss quadrature.

If q is the solution of the system (34), (36) and the piecewise constant approximation q_h given by the solution of (52), then we have the following error bounds (see [23]):

$$\|q - q_h\|_{H^{-1/2}(\Gamma)} \leq C_1 h \|q\|_{H^1(\Gamma)}, \tag{57}$$

and if ξ_h is the approximation of (33) then

$$\left\| \frac{\partial \xi}{\partial \nu} - \frac{\partial \xi_h}{\partial \nu} \right\|_{H^{-1/2}(\Gamma)} \leq C_2 h \|q\|_{H^1(\Gamma)}. \tag{58}$$

The approximation of the normal derivative $\frac{\partial \xi}{\partial \nu}$ at $x_l \in \ell_l$ is given by:

$$\frac{\partial \xi_h}{\partial \nu}(x_l) = -\frac{1}{2\pi} \sum_{\substack{i=1 \\ i \neq l}}^{n} q_i \sum_{m=1}^{K} p_m \frac{\partial \ln \|x_l - x_i(s_m)\|}{\partial \nu}$$

$$+\frac{1}{2}q_l, \tag{59}$$

where $x_i(s_m)$ are the integration points and p_m the weights of the Gauss quadrature formula. Thus, the computation of $\frac{\partial \xi_h}{\partial \nu}(x_l)$ needs $O(n)$ floating point operations.

Equilibrium equation

Consider a direction $\hat{V}^i \in \mathbb{R}^2$ associated to each vertex x_i of Γ^h and the continuous piecewise linear vector field V^i from Γ^h in $\mathbb{R}^2$ such that $V^i(x_k) = \delta_{ik}\hat{V}^i$. If we project the equation (44) in the finite dimensional space generated by V^i, $i \in \{1, \ldots, n\}$, the discrete version of the equilibrium is the following:

$$\begin{aligned} &DE_i(\boldsymbol{u}_p, \boldsymbol{u}, \boldsymbol{q}) = \\ &= \int_{\Gamma_{\boldsymbol{u}}} \left(\frac{1}{2\mu_0} \left| \frac{\partial \varphi_\omega}{\partial \nu} \right|^2 \right) (V^i \cdot \nu)\, d\gamma \\ &+ \int_{\Gamma_{\boldsymbol{u}}} (-p_0)\, (V^i \cdot \nu)\, d\gamma + \sigma \mathcal{C}^i \cdot \hat{V}^i \quad , \end{aligned} \tag{60}$$

where $i \in \{1, \ldots, n\}$ and $\mathcal{C}^i$ is an approximation of the mean curvature at x_i, given by:

$$\mathcal{C}^i = \left(\frac{(x_i - x_{i-1})}{\|x_i - x_{i-1}\|} - \frac{(x_{i+1} - x_i)}{\|x_{i+1} - x_i\|} \right). \tag{61}$$

The gradient $\nabla\varphi$ is computed using (37), (38) and (39).

In the case of equation (48), we consider a piecewise linear function p_h defined as:

$$p_h(x) = \sum_{i=1}^{n} p_i f_i, \tag{62}$$

where the function f_i satisfies $f_i(x_k) = \delta_{ik}$. Then, defining $\boldsymbol{p}^T = (p_1, \ldots, p_n)$, the equilibrium equation is defined as:

$$\begin{aligned} &DF_i(\boldsymbol{u}_p, \boldsymbol{p}, \boldsymbol{q}) = \\ &= \int_{\Gamma^*} \left(\frac{1}{2\mu_0} \left| \frac{\partial \varphi_\omega}{\partial \nu} \right|^2 \right) (V^i \cdot \nu)\, d\gamma \\ &+ \int_{\Gamma^*} (-p_0 + p_h)\, (V^i \cdot \nu)\, d\gamma + \\ &+ \sigma \mathcal{C}^i \cdot \hat{V}^i. \end{aligned} \tag{63}$$

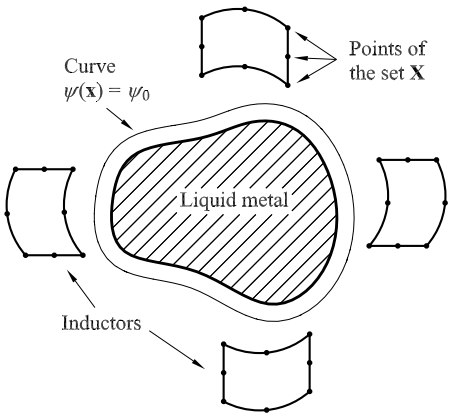

Figure 3. Geometric constraints.

Geometric constraints

In order to avoid the possibility of overlapping between the domains occupied by the liquid metal and the inductors, we consider the following inequality constraints:

$$\psi(x_j) \leq \psi_0, \quad \text{for all } x_j \in \boldsymbol{X}, \tag{64}$$

where $\boldsymbol{X}$ is a chosen set of points belonging to the boundary of the inductors. The real valued function ψ is zero in the interior of the liquid metal and negative in the exterior. Then, choosing a negative value for the parameter ψ_0, (64) enforces the points x_j to be in the exterior of the liquid metal as illustrated by Fig. 3.

The function ψ that we propose is defined as the solution of:

$$\begin{aligned} \Delta\psi(x) &= 0 \qquad \text{in } \Omega^*, \\ \psi(x) &= 0 \qquad \text{on } \Gamma^*, \\ \int_{\Gamma^*} \nabla\psi(x) \cdot \nu\, d\gamma &= -1. \end{aligned} \tag{65}$$

In a similar way as the function ξ in Section , ψ can be calculated as:

$$\psi(x) = -\frac{1}{2\pi} \int_\Gamma q(y) \ln \|x - y\|\, d\gamma + c, \tag{66}$$

where q must satisfy:

$$\int_\Gamma q(y)\, d\gamma = -1. \tag{67}$$

As in Section , an approximated solution of q and c can be obtained solving a linear system similar to

(52). The numerical approximation of the function ψ is obtained employing (66).

The value ψ_0 can be defined choosing a point in the exterior of the liquid metal and calculating the value of the function ψ at this point.

Defining $\boldsymbol{h}_j(\boldsymbol{u}_p) = \psi(x_j(\boldsymbol{u}_p)) - \psi_0$, all the geometric constraints are expressed as:

$$\boldsymbol{h}(\boldsymbol{u}_p) \leq 0. \tag{68}$$

Note that the function ψ was defined for the fixed domain Ω^*. Then, strictly speaking, the constraints (64) are suitable just for the the second formulation of the inverse problem. In the case of the first formulation, ψ should be defined for the changing domain Ω_Z. In that case there is an extra computational cost associated to the computation of q and c each time that the domain Ω_Z is updated. However, we have observed for all the examples considered that the use of ψ defined for the fixed domain Ω^* is enough to prevent the overlapping between domains. The reason is that the domain occupied by the liquid metal keeps very close to the target shape all along the optimization process.

NUMERICAL EXAMPLES

We consider several examples to illustrate the behavior of the proposed formulations of the inverse problem. The shape and the surface S_0 of the target shape, the surface tension σ, the intensity I and the dimensionless coefficients α_p are given. For each example all the parameters, including the parameters ψ_0 of the geometric constraints, are the same for both formulations. The initial values of the state variables $\boldsymbol{q}$ and p_0, the shape variable $\boldsymbol{u}$ of the first formulation and the pressure $\boldsymbol{p}$ of the second one are set equal to zero for all the examples.

For the solution of the optimization problems, the line search interior-point algorithm for nonlinear constrained optimization problems FAIPA was employed. For a given feasible point with respect to the inequality constraints, FAIPA defines a feasible and descent arc solving three linear systems of equations with the same coefficient matrix. Then, it performs a line search along this arc to define the next point. FAIPA makes subsequent iterations until a convergence criterion is satisfied.

At each iteration FAIPA needs the vector of partial derivatives with respect to all the design variables of the objective function and all the constraints. Herein, we have calculated exact derivatives for all the functions of the discretized model. For more details about FAIPA see [10, 11, 24].

For each example we plot the initial inductors, the target shape of the liquid metal, the inductors obtained by the optimization algorithm and the evolution of the objective function during the iterative process.

Example 1

The target shape of this example is the solution of the direct free-surface problem considering four concentrated intensities of value $I = 0.1$, with the sign given by Fig. 4, and an area S_0 equal to π; see Example $1a$ in [6].

For the inverse problem we consider four inductors. The intensity I is equal to 0.1 and the surface tension σ is equal to 1.0×10^{-4}. The dimensionless coefficients α_p have absolute value equal to 4.0 with the sign given by Fig. 4. Solutions for the first formulation and three different values of the penalty parameter r are given by Fig. 5. For the second formulation, the solutions are given by Fig. 7. The evolution of the objective functions throughout the optimization process are shown in Figs. 6 and 8.

Example 2

The target shape of this example is the bar of area S_0 equal to 7.86 depicted by Fig. 9. For the inverse problem we consider twelve inductors. The intensity I is equal to 0.1 and the surface tension σ is equal to 1.0×10^{-4}. The dimensionless coefficients α_p have absolute value equal to 4.0 with the sign given by Fig. 9. Solutions for the first formulation and three different values of the penalty parameter r are given by Fig. 10. For the second formulation, the solutions are given by Fig. 12.

Example 3

The target shape of this example is the bar of area S_0 equal to 4.99 depicted by Fig. 14. For the inverse problem we consider twelve inductors. The intensity I is equal to 0.1 and the surface tension σ is equal to 1.0×10^{-4}. The dimensionless coefficients α_p have absolute value equal to 4.0 with the sign given by Fig. 14. Solutions for the first formulation and three different values of the

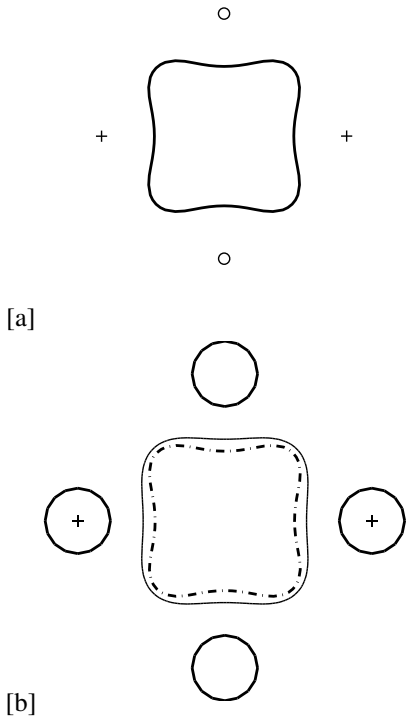

[a]

[b]

Figure 4. Example 1 - Target shape and initial configuration. (a) Equilibrium shape considering concentrated intensities. Solid line: equilibrium shape, pluses: positive currents, circles: negative currents. (b) Initial configuration. Circles with pluses: inductors of positive current, circles without pluses: inductors of negative current. Dash-dotted line: target shape. Thin solid line: geometric constraint.

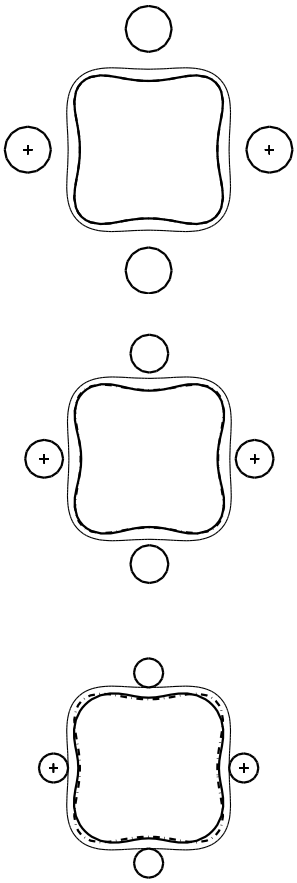

[a]

[b]

[c]

Figure 5. Example 1 - Solutions of the first formulation. (a) Solution for $r = 0$. (b) Solution for $r = 5$. (c) Solution for $r = 100$. Solid line: equilibrium shape, pluses: positive currents, circles: negative currents. (b) Initial configuration. Circles with pluses: inductors of positive current, circles without pluses: inductors of negative current. Dash-dotted line: target shape. Thick solid line: equilibrium shape. Thin solid line: geometric constraint.

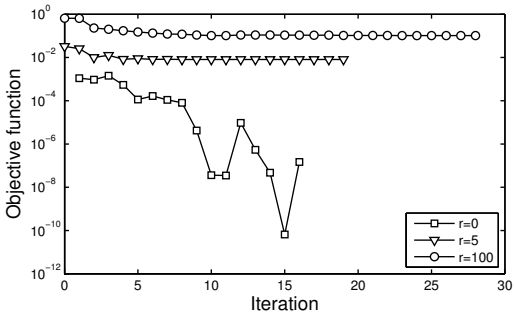

Figure 6. Example 1 - Evolution of the objective function, first formulation.

penalty parameter r are given by Fig. 15. For the second formulation, the solutions are given by Fig. 17.

CONCLUSIONS

This paper deals with the shape design of the inductors used in the electromagnetic casting of molten metals. Two different approaches based on nonlinear optimization have been proposed in order to find the position and shape of suitable inductors. The first one minimizes the difference between the geometries of the best possible equilibrium domain and the target shape; the second minimizes a slack variable function related to the equilibrium equation on the target boundary.

It was also considered the addition of a regularizing term to the objective function, in order to penalize the solutions presenting a high magnetic field vector on the boundary of the liquid metal. This regularizing term have a "smoothing" action needed, because the computed magnetic field must correspond with an analytic Γ, if a solution $\boldsymbol{B}$ is to exist.

The finite dimensional optimization problems obtained after discretization were solved employing the line search interior-point algorithm FAIPA.

Some exhibited examples show that both formulations are effective to design suitable inductors.

ACKNOWLEDGEMENTS

The authors thank the Brazilian Research Councils CAPES, CNPq and Faperj for the financial support. The first author thanks the National Research and Innovation Agency (ANII) of Uruguay

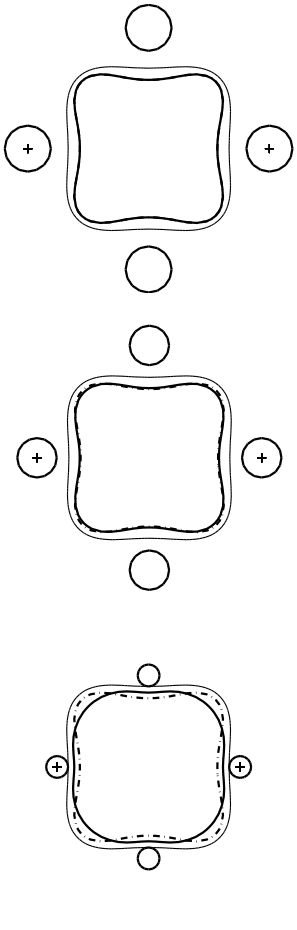

Figure 7. Example 1 - Solutions of the second formulation. (a) Solution for $r = 0$. (b) Solution for $r = 0.0001$. (c) Solution for $r = 0.0005$. Solid line: equilibrium shape, pluses: positive currents, circles: negative currents. (b) Initial configuration. Circles with pluses: inductors of positive current, circles without pluses: inductors of negative current. Dash-dotted line: target shape. Thin solid line: geometric constraint.

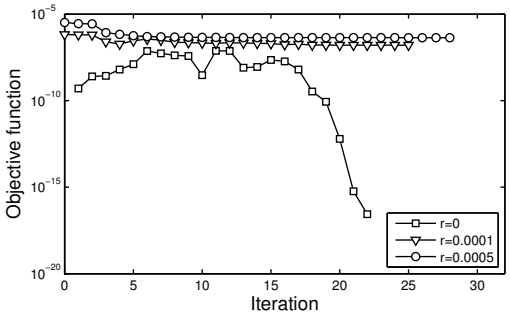

Figure 8. Example 1 - Evolution of the objective function, second formulation.

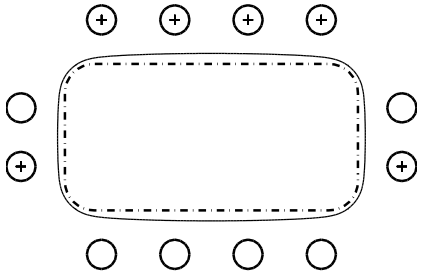

Figure 9. Example 2 - Target shape and initial configuration. Circles with pluses: inductors of positive current, circles without pluses: inductors of negative current. Dash-dotted line: target shape. Thin solid line: geometric constraint.

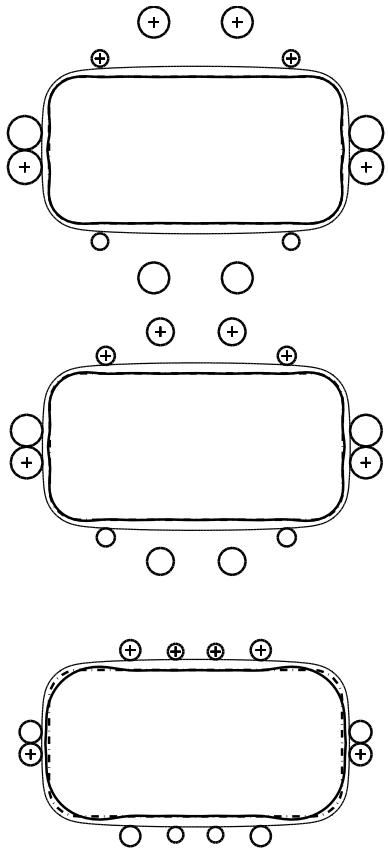

[a]

[b]

[c]

Figure 10. Example 2 - Solutions of the first formulation. (a) Solution for $r = 0$. (b) Solution for $r = 5$. (c) Solution for $r = 100$. Circles with pluses: inductors of positive current, circles without pluses: inductors of negative current. Dash-dotted line: target shape. Thick solid line: equilibrium shape. Thin solid line: geometric constraint.

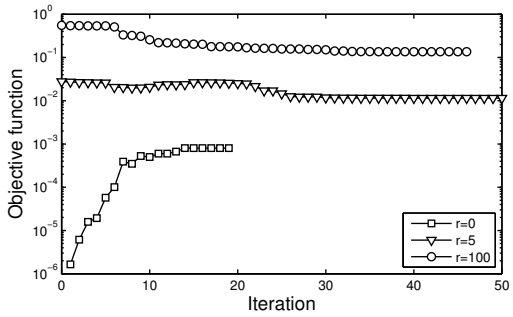

Figure 11. Example 1 - Evolution of the objective function, first formulation.

for the financial support. The second author thanks the French Research Councils COFECUB, INRIA and CNRS for the financial support.

REFERENCES

[1] H. K. Moffat, Magnetostatic equilibria and analogous Euler flows of arbitrarily complex topology. I. Fundamentals, J. Fluid Mech. ,159, p. 359, (1985)

[2] J. A. Shercliff, Magnetic shaping of molten metal columns, Modèlisation mathématique et analyse numérique, Proc. R. Soc. Lond., A 375, p. 455, (1981)

[3] A. Henrot, J.-P. Brancher and M. Pierre, Existence of equilibria in electromagnetic casting, Proceedings of the Fifth International Symposium on Numerical Methods in Engineering, Vol. 1, 2 , Lausanne, 1989, p. 221.

[4] A. Henrot and M. Pierre, Un problème inverse en formage de mètaux liquides, Modèl. Math. Anal. Numér, 23, p. 155, (1989)

[5] T. P. Felici and J.-P. Brancher, The inverse shaping problem, European J. Mech. B Fluids, 10, 5, p. 501, (1991)

[6] A. Canelas, J. R. Roche and J. Herskovitz, The inverse electromagnetic shaping problem, Struct. Multidiscip. Optim., 38, 4, p. 389, (2009)

[7] A. Canelas, J. R. Roche and J. Herskovitz, Inductor shape optimization for electromag-

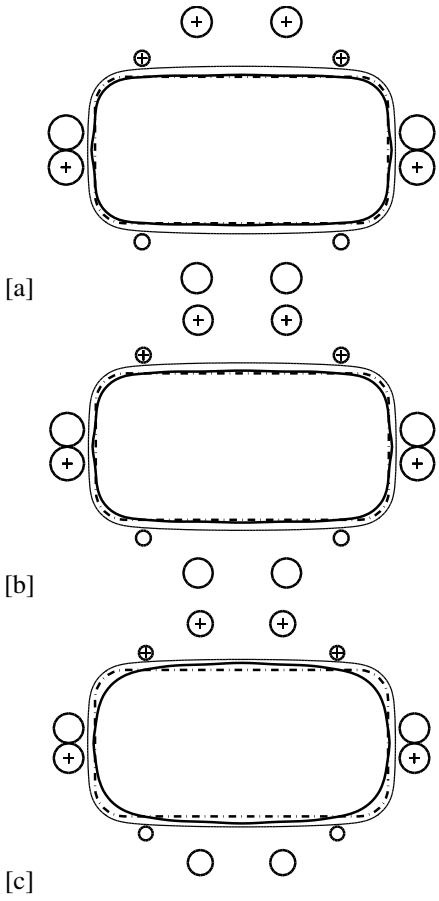

Figure 12. Example 2 - Solutions of the second formulation. (a) Solution for $r = 0$. (b) Solution for $r = 0.00002$. (c) Solution for $r = 0.0001$. Circles with pluses: inductors of positive current, circles without pluses: inductors of negative current. Dash-dotted line: target shape. Thick solid line: equilibrium shape. Thin solid line: geometric constraint.

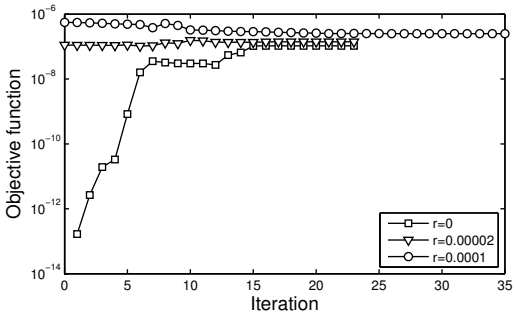

Figure 13. Example 1 - Evolution of the objective function, second formulation.

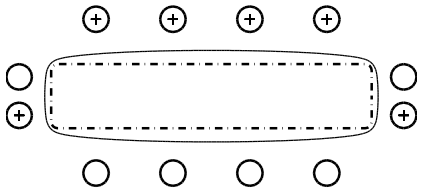

Figure 14. Example 3 - Target shape and initial configuration. Circles with pluses: inductors of positive current, circles without pluses: inductors of negative current. Dash-dotted line: target shape. Thin solid line: geometric constraint.

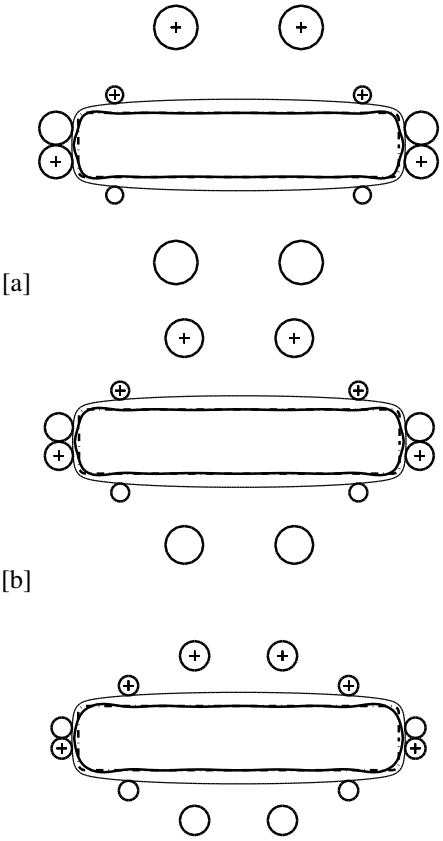

[a] [b] [c]

Figure 15. Example 3 - Solutions of formulation 1. (a) Solution for $r = 0$. (b) Solution for $r = 2$. (c) Solution for $r = 10$. Circles with pluses: inductors of positive current, circles without pluses: inductors of negative current. Dash-dotted line: target shape. Thick solid line: equilibrium shape. Thin solid line: geometric constraint.

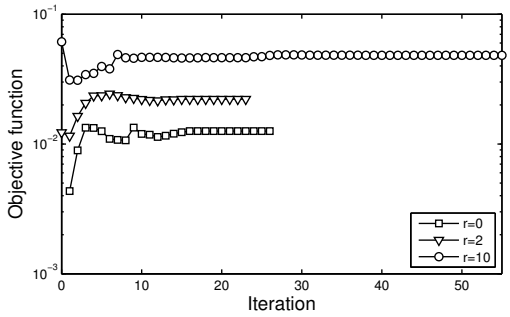

Figure 16. Example 1 - Evolution of the objective function, first formulation.

netic casting, Struct. Multidiscip. Optim., 39, 6, p. 589, (2009)

[8] R. T. Haftka and M. P. Kamat, Simultaneous nonlinear structural analysis and design, Comput. Mech., 4, 6, p. 409, (1989)

[9] A. Canelas, J. Herskovits and J. C. F.Telles, Shape Optimization using the Boundary Element Method and a SAND Interior Point Algorithm for Constrained Optimization, Comput. & Structures, 86, 13–14, p. 1517, (2007)

[10] J. Herskovits, Feasible direction interior-point technique for nonlinear optimization, J. Optim. Theory Appl., 99, 1, p. 121, (1998)

[11] J. Herskovits, P. Mappa, E. Goulart and C. M. Mota Soares, Mathematical programming models and algorithms for engineering design optimization, Comput. Methods Appl. Mech. Engrg., 194, 30-33, p. 3244, (2005)

[12] J.-P. Brancher and O. E. Séro-Guillaume,Étude de la déformation d'un liquide magnétique, Arch. Rational Mech. Anal., 90, 1, p. 57, (1985)

[13] A. Gagnoud, J. Etay and M. Garnier, Le probléme de frontiére libre en lévitation électromagnétique, J. Méc. Théor. Appl., 5, 6, p. 911, (1986)

[14] A. Novruzi and J. R. Roche, Second Order Derivatives, Newton Method, Application

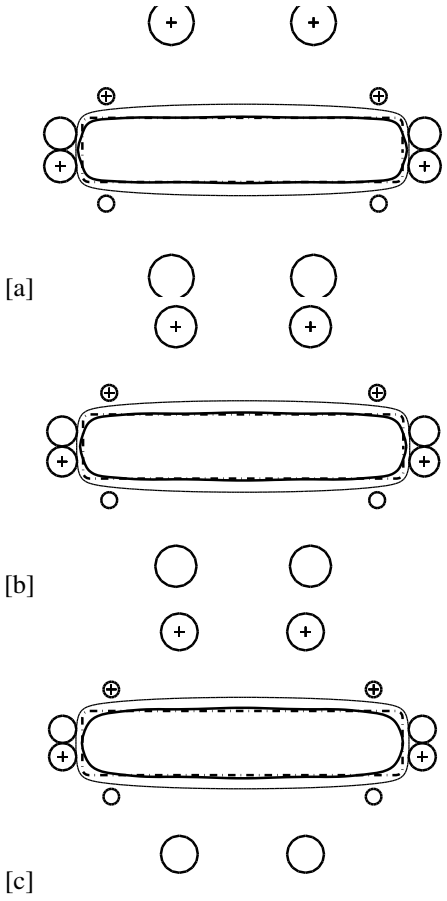

Figure 17. Example 3 - Solutions of formulation 2. (a) Solution for $r = 0$. (b) Solution for $r = 0.00005$. (c) Solution for $r = 0.0001$. Circles with pluses: inductors of positive current, circles without pluses: inductors of negative current. Dash-dotted line: target shape. Thick solid line: equilibrium shape. Thin solid line: geometric constraint.

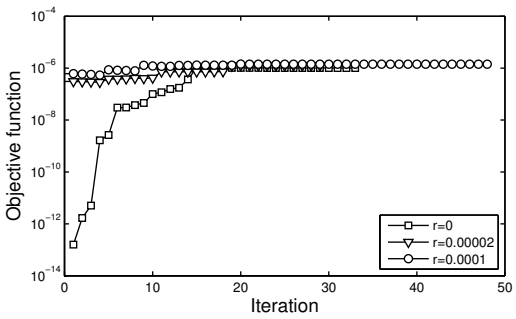

Figure 18. Example 1 - Evolution of the objective function, second formulation.

to Shape Optimization, RR-2555, INRIA, (1995)

[15] M. Pierre and J. R. Roche, Computation of free surfaces in the electromagnetic shaping of liquid metals by optimization algorithms, European J. Mech. B Fluids, 10, 5, p. 489, (1991)

[16] M. Pierre and J. R.Roche, Numerical simulation of tridimensional electromagnetic shaping of liquid metals, Numer. Math., 65, 2, p. 203, (1993)

[17] G. Allaire, Conception Optimale de Structures, Mathématiques and Applications, 58, Springer-Verlag, Berlin, 2007.

[18] S. Murat and J. Simon, Sur le contrôle par un domaine géométrique, 76015, Laboratoire d'Analyse Numérique, Université de Paris, (1976)

[19] J. Simon, Differentiation with respect to the domain in boundary value problems, Numer. Funct. Anal. Optim., 2, 7-8, p. 649, (1981)

[20] A. Novruzi and M. Pierre, Structure of shape derivatives, J.Evo.Equ., 2, p. 365, (2002)

[21] R. Kress, Linear integral equations, Applied Mathematical Sciences, 82, Springer-Verlag, New York, 1999.

[22] C. R. Sullivan, Optimal Choice for Number of Strands in a Litz-Wire Transformer Winding, IEEE Trans. Power Electron., 14, 2, p. 283, (1999)

[23] J. C. Nédélec, Approximation des équations intégrales en mécanique et en physique, Centre de mathématiques appliquées -Ecole Polytechnique, (1977)

[24] J. Herskovits, E. Laporte, P. Le Tallec and G. Santos, A quasi-Newton interior point algorithm applied to constrained optimum design in computational fluid dynamics, Rev. Européenne Élém. Finis, 5-6, p. 595, (1996)